

PACS 61.72.V, 73.40

Nanostructuring the SiO_x layers by using laser-induced self-organization

O.V. Steblova¹, L.L. Fedorenko², A.A. Evtukh²

¹Taras Shevchenko Kyiv National University, Institute of High Technologies,
Kyiv, Ukraine, e-mail: steblovia@gmail.com

²V. Lashkaryov Institute of Semiconductor Physics NAS of Ukraine,
41, prospect Nauky, 03680 Kyiv, Ukraine; e-mail: leonfdrn@gmail.com

Abstract. The processes of laser-induced transformation of SiO_x oxide layers into the nanocomposite ones were studied. The possibility of phase separation in the form of Si nanocrystals surrounded by corresponding SiO₂ oxide matrix under irradiation by nanosecond pulses of YAG:Nd⁺³-laser were shown. Laser radiation at the fundamental wavelength, $\lambda_1 = 1064$ nm, and second harmonic, $\lambda_2 = 532$ nm, were applied at researches. The size and surface concentration of nanofragments dependences on the intensity and wavelength of the laser irradiation have been determined from experimental data based on atomic force microscopy, infrared transmission spectra and electro-physical measurements. SiO_x nanocomposite layers containing Si nanoparticles, the size of which depends on laser beam intensity and wavelength, have been obtained. The processes of nanoparticles formation occur mainly through generation and mass transfer of interstitial atoms in the solid mode (before the melting point threshold) due to the effect of laser thermal shock.

Keywords: nanocrystal, oxides, nanocomposite, laser thermal shock, mass transfer.

Manuscript received received 01.02.17; revised version received 10.04.17; accepted for publication 14.06.17; published online 18.07.17.

1. Introduction

Structures with silicon nanoparticles that are grown inside SiO₂ draw researchers' attention due to prospects of creation on their basis functionally new nano-electronic devices such as nanocrystal memory [1, 2], single-electron transistors [3], Si-based LEDs and laser [4-6]. The fabrication route of Si nanocrystal formation generally consists of two steps. First, SiO_x films are made either by deposition [7-12], or by implanting Si atoms into pure silica [6]. Then, nc-Si is obtained by thermal annealing of the layers in the inert (argon or nitrogen) atmosphere. The size distribution and number of Si nanocrystals were found to strongly depend both on the content of excess Si into SiO_x films and on annealing temperature and duration. The laser annealing for transformation of SiO_x film into the nanocomposite one containing Si nanoclusters in a SiO₂ matrix are investigated as an alternative annealing method [12-18].

Among the newest technologies of recent years, the direction of laser induced nanostructuring is intensively

developed as non-destructive method for relatively soft technological impact. At the same time, the increased interest in nanostructuring the oxides is explained by the possibility of their transformation into nanocomposite layers containing nanocrystals surrounded by corresponding oxide matrix. For example, Zn nanocrystals in the ZnO matrix [19], Ti in TiO₂, Si in SiO₂ matrix [20]. It is already known from literature, including our work [16], that there are experiments demonstrating the possibility of non-ablative laser-stimulated phase separation of SiO_x oxide film (Si-enriched silicon oxide) with appearance of Si nanoclusters and SiO₂ oxide matrix at laser intensities close to the threshold point, but non-destructive for the SiO_x/Si system.

In case of thermal annealing the Si nanocrystals are formed over all the area substrate. The laser annealing with intensities lower than the destruction threshold has been used here for the creation of structures with silicon nanoclusters on local areas of wafer. The influence of

laser intensity on SiO_x film structure transformation and its electrical properties are presented.

2. Experimental

The SiO_x/Si structures were obtained by ion plasma sputtering (IPS) of Si target in O₂+Ar ambient on single crystalline Si substrate (*n*-type, $\rho = 4.5 \text{ Ohm}\cdot\text{cm}$ (100)). The thickness of SiO_x film was $d = 100 \text{ nm}$ and stoichiometry index was $x = 0.98$. Investigations of the changes of surface morphology, structural, optical and electrical properties of the SiO_x/Si system were performed before and after laser irradiation. The atomic force microscopy (AFM) (Nanoscope IIIa, Digital Instruments, Santa-Barbara, IR Fourier spectrometer BX (firm Perkin-Elmer) in the frequency range of 800...1400 cm⁻¹, scanning electron microscope (SEM) (TescanMira) using 15 kV electron beam, optical microscope Nikon LV150 were used for investigations of the films. The standard YAG:Nd³⁺-laser with the base frequency $\lambda = 1064 \text{ nm}$ and second harmonic $\lambda = 532 \text{ nm}$ were used as an irradiation source.

Laser irradiation was carried out at the room temperature and atmospheric pressure. The samples with the Si/SiO_x structures were irradiated from the SiO_x side using the fundamental ($\lambda = 1064 \text{ nm}$, $\tau = 15 \text{ ns}$) and the second harmonic ($\lambda = 532 \text{ nm}$, $\tau = 10 \text{ ns}$) frequencies of the YAG:Nd³⁺ laser in the Q-modulation mode with the intensity in the range from 10 to 110 MW/cm². This range of intensities was chosen to achieve a non-destructive annealing of SiO_x layer using Si substrate as a heat source. Laser irradiation with the wavelength used is not adsorbed by the SiO_x film but mainly by Si, and, in such a way, it heated the substrate. In this case, the Si substrate is a heat source for the film. The total influence of laser beam on local place was $\tau = 15 \text{ ns}$ and $\tau = 10 \text{ ns}$ in case of $\lambda = 1064 \text{ nm}$ and $\lambda = 532 \text{ nm}$, correspondingly. The level of the laser beam intensity was controlled by defocusing and/or by the neutral grey optical filters. The pulse laser energy and duration were measured using a conventional pulse energy meter and coaxial photo-element with oscilloscope.

3. Laser-stimulated phase separation of the SiO_x/Si structure

The fact of nanofragmentation of the SiO_x film is confirmed by correlation between formation of nanofragments on the surface of SiO_x/Si structure (see AFM image in Fig. 1b) and a shortwave shift of the IR transmission spectrum minimum from 1032 to 1073 cm⁻¹ (Fig. 2). As seen from Fig. 2, the intensity of IR spectrum minimum increases with shifting into the high-frequency region, and absorption area becomes wider after the laser annealing. The shift of minimum position from $\nu_{m1} = 1032 \text{ cm}^{-1}$ ($x = 0.98$) to $\nu_{m2} = 1073 \text{ cm}^{-1}$ ($x = 1.76$) is observed. This shift of the frequency minimum is indicative of phase separation and transformation of the SiO_x film [21]. As a result of the structure transformation, the film properties are significantly changed.

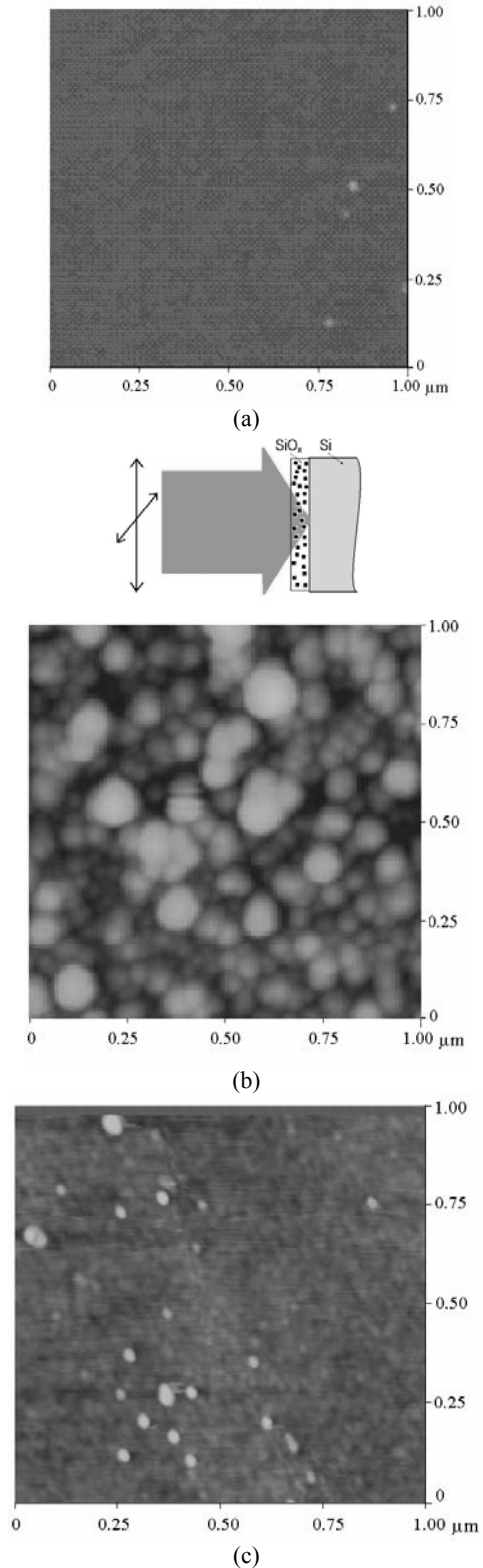


Fig. 1. AFM image of SiO_x-film surface morphology before (a) and after laser (b, c) annealing with the irradiation intensity $I = 16 \text{ MW/cm}^2$: b) $\lambda_1 = 1064 \text{ nm}$, $h = 85 \text{ nm}$ and c) $\lambda_2 = 532 \text{ nm}$, $h = 5 \text{ nm}$, $n_{\text{Si}} = 2.7 \cdot 10^{10} \text{ cm}^{-2}$ ($\alpha_1 = 10 \text{ cm}^{-1}$, $\alpha_2 = 10^4 \text{ cm}^{-1}$). $I_{th.in}(\lambda_1) = 14 \text{ MW/cm}^2$, $I_{th.in}(\lambda_2) = 6 \text{ MW/cm}^2$; $I_{th.dam}(\lambda_1) = 114 \text{ MW/cm}^2$, $I_{th.dam}(\lambda_2) = 54 \text{ MW/cm}^2$ ($I_{th.in}$ is the light intensity for beginning of morphology changes; $I_{th.dam}$ is the light intensity for destructive damage).

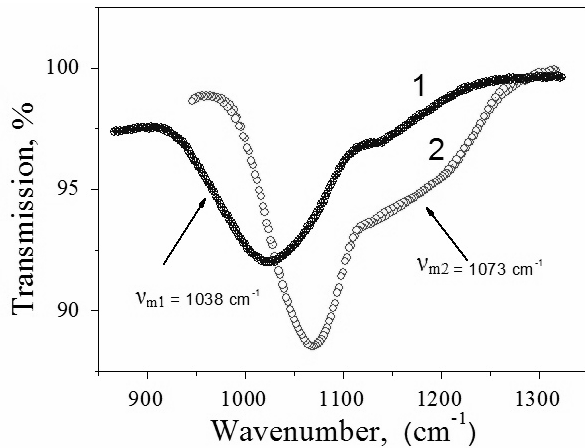


Fig. 2. IR transmission spectra of SiO_x film ($x = 0.98$) before (1) and after (2) laser annealing at the intensity $I = 100 \text{ MW/cm}^2$ ($\lambda_2 = 1064 \text{ nm}$).

The detail analysis of IR spectra was performed being based on the mathematical decomposition of the optical density band by elements of the Gaussian profile. It was shown that the main absorption band of the initial SiO_x film consists of seven elementary sub-bands resulting from transverse (TO mode) and longitudinal (LO mode) valence oscillations of bridging oxygen that is the part of the molecular complexes $\text{Si-O}_y\text{-Si}_{4-y}$ ($1 \leq y \leq 4$) (Fig. 3). The main contribution to the IR absorption band of the initial film is given by the sub-bands 1, 2, 3, 4, 5 that correspond to complexes of unoxidized silicon (Si-O-Si_3 , $\text{Si-O}_2\text{-Si}_2$, $\text{Si-O}_3\text{-Si}$). Such spectral distribution is kept up to the first threshold of intensity (14 MW/cm^2).

As a result of laser annealing at the intensity $I \geq 14 \text{ MW/cm}^2$ ($\lambda_1 = 1064 \text{ nm}$), the initial silicon-enriched SiO_x ($x = 0.98$) film begins to transform into the nanocomposite $\text{SiO}_x(\text{Si})$ film. After irradiation with

the intensity $I = 100 \text{ MW/cm}^2$, the stoichiometric index becomes $x \approx 1.76$, and significant redistribution of elementary band intensities is observed. The integrated intensity of the sub-band associated with Si-O-Si_3 complexes decreased by 6.5 times, and sub-bands associated with the $\text{Si-O}_2\text{-Si}_2$, $\text{Si-O}_3\text{-Si}$ complexes disappeared. The relative area of sub-bands caused by Si-O TO vibration modes from the SiO_4 tetrahedron combined into 4- and 6-fold rings is approximately 68%, and the area of Si-O-Si sub-band is 14.6% of the total spectrum area indicating formation of SiO_2 phase regions, which correlates with appearance of nano-Si crystals on the surface.

Irradiation with the YAG:Nd^{+3} laser at two wavelengths $\lambda_1 = 1064 \text{ nm}$ and $\lambda_2 = 532 \text{ nm}$ was applied in this experiment. At the high intensity level of the fundamental wavelength ($\lambda_1 = 1064 \text{ nm}$), the substrate (Si) was mainly heated, in the second case ($\lambda_2 = 532 \text{ nm}$) as substrate as well as SiO_x film was heated. In both cases, the effect of intensive formation of the nanostructure was carried out. In the first case ($\lambda_1 = 1064 \text{ nm}$), the intensive formation of nanoparticles begin at the light intensity $I = 16 \text{ MW/cm}^2$ with the average cross-section diameter $d = 70 \text{ nm}$ and the height $h = 85 \text{ nm}$ (Fig. 1b). In the second case ($\lambda_2 = 532 \text{ nm}$), with the same I values, $d = 7 \text{ nm}$ and $h = 5 \text{ nm}$ were obtained (Fig. 1c).

The thresholds of beginning of the morphology changes were sufficiently different: $I_{th1} = 14 \text{ MW/cm}^2$ and $I_{th2} = 6 \text{ MW/cm}^2$ for $\lambda_1 = 1064 \text{ nm}$ and $\lambda_2 = 532 \text{ nm}$, accordingly. Besides, the destructive damage thresholds were also significantly different: $I_{th1} = 114 \text{ MW/cm}^2$ and $I_{th2} = 54 \text{ MW/cm}^2$. It is connected with the large difference between the absorption coefficients ($\alpha_1 = 10 \text{ cm}^{-1}$, $\alpha_2 = 10^4 \text{ cm}^{-1}$) for two laser wavelengths ($\lambda_1 = 1064 \text{ nm}$, $\lambda_2 = 532 \text{ nm}$), accordingly, at least, at not very high intensity levels.

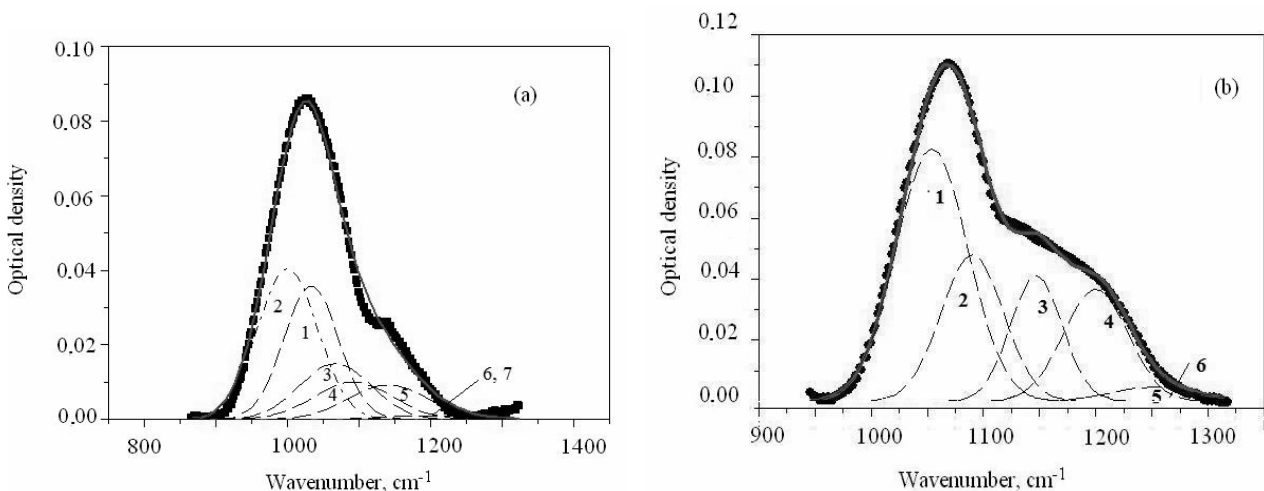


Fig. 3. Mathematical decomposition of optical density bands of oxide films by Gaussian shape components: a) the initial sample ($x = 0.98$); b) the sample annealed with the laser intensity 100 MW/cm^2 ($x = 1.76$).

As a rule, there is a tendency in nanocrystal size growth with increasing of the intensity (for example: $\lambda_1 = 1064$ nm: $I = 16$ MW/cm², $h = 85$ nm; $I = 110$ MW/cm², $h = 100$ nm; $\lambda_2 = 532$ nm: $I = 16$ MW/cm², $h = 5$ nm; $I = 50$ MW/cm², $h = 30$ nm).

In case of stationary illumination at the wavelength $\lambda_1 = 1064$ nm, the temperature of the surface is lower, and the size of nanoclusters, as it is expected, has to be smaller in comparison with that under illumination at $\lambda_2 = 532$ nm. But in our experiments with nanosecond pulse illumination, there is a non-stationary process, and the role of temperature and pressure gradients is critical. The mechanism of Si nanocrystals formation is as follows. Because the pulsed laser irradiation leads to rapid and non-homogeneous heating the sample, the concentration of interstitial Si grows on the surface through the generation and redistribution of an excessive Si_i due to the effect of laser thermal shock [22-24]. Laser thermal shock effect manifests itself in certainty of the transfer direction of the impurity atoms or defects in the crystal lattice under conditions of temperature dT/dx and pressure dP/dx gradients action. The transfer direction depends on the ratio of the covalent radii of impurity atom to that of the basic substance atoms. The force acting on the atom is:

$$F = -ak \times \frac{\partial T}{\partial x'}, \quad a \approx k \left(1 - \frac{\rho'}{\rho} \right), \quad (1)$$

where ρ , ρ' are the covalent radii of substance and defect atoms, accordingly.

The atoms with larger covalent radius, as it follows from (1), move to a maximum temperature in the field of gradients of temperature and pressure, created by laser irradiation, while smaller atoms move against the gradient (to lower temperatures) (Fig. 4). As a result, the layer or island enriched with Si_i is formed on the surface.

The results on influence of laser annealing on the conductivity of SiO_x films are illustrated in Fig. 5, where the current density on the intensity of laser irradiation ($T = 300$ K) with electric field as a parameter are shown.

At the beginning, the increase in current density with growth of laser irradiation intensity to $I = 17$ MW/cm² is observed. The analysis of IR spectra has been shown that after annealing at $I = 10$ MW/cm² the structure, in comparison with the original film, wasn't changed. The electron traps in the film are the conduction states [25]. The decline in current density is observed with increasing the intensity of laser irradiation from 17 to 35 MW/cm². It is caused by the fact that the additional silicon-oxygen bonds are formed with the growing intensity, the concentration of Si-O₂-Si₂, Si-O₃-Si complexes are reduced and, as a result, the density of electron traps are decreased [26].

Within the range $35 < I < 50$ MW/cm² the current density is almost unchanged. At this stage of laser annealing, the phase of stoichiometric silicon oxide SiO₂ are formed. This phase is represented by complexes of SiO₄ tetrahedrons combined into 4- and 6-fold rings, and Si nanocrystals [21, 26]. As a result of these changes, the higher density of the interface states between SiO₂ and Si nanocrystals has been appeared, and the number of conductive states in the amorphous SiO_x matrix are reduced. Beginning from $I \geq 50$ MW/cm², the conductivity has been increased. The reason for this current behavior is the further structural transformations that lead to the tunnel mechanism of electron transport through Si nanocrystals.

As been determined, the basic mechanisms of conductivity through SiO_x films after laser annealing are the electron hopping with variable length (the Mott law), space-charge limited current (SCLC), Pool-Frenkel conductivity, and Fowler-Nordheim tunneling in dependence on measurement temperature and electric field [27].

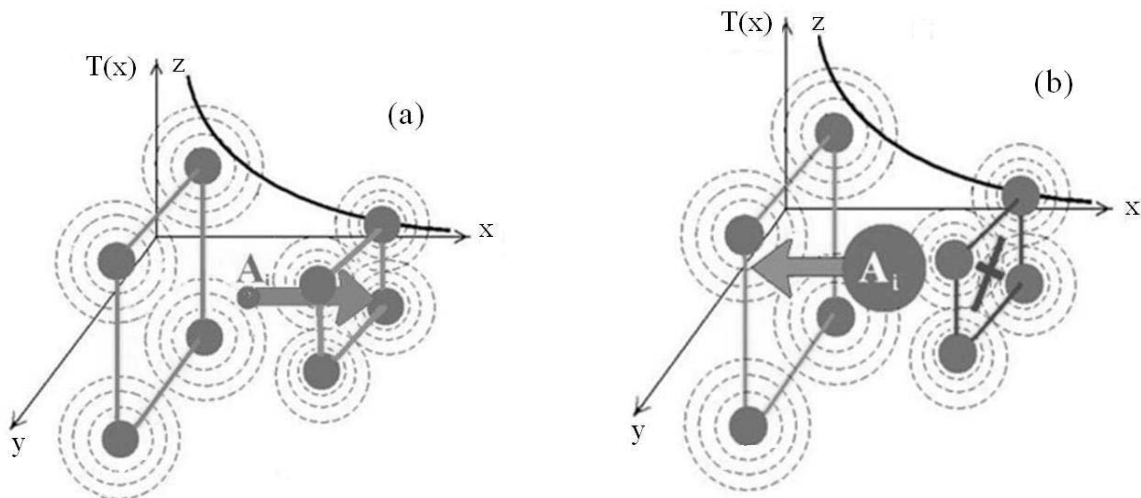


Fig. 4. Illustration of the mass-transfer in conditions of the laser thermal shock effect: a) $\rho_{im} < \rho_{bm}$, b) $\rho_{im} > \rho_{bm}$, $\rho_{Si} = 1.17$ Å, $\rho_O = 0.66$ Å (ρ_{im} is the radius of impurity atom, ρ_{bm} is the radius of a base material atom).

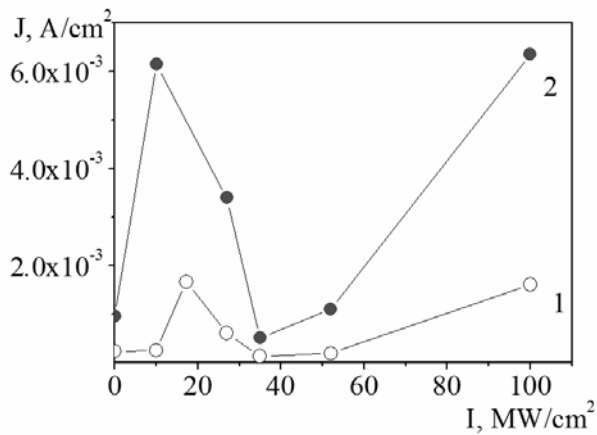


Fig. 5. The dependences of the current density through SiO_x film on the laser irradiation intensity ($\lambda_1 = 1064$ nm, $t = 10$ ns) at fixed values of the electric field: 1 – $E = 2 \cdot 10^5$ V/cm, 2 – $E = 4 \cdot 10^5$ V/cm.

4. Conclusions

The possibility of laser-induced nanostructuring of the SiO_x oxide has been shown. The average size of nanoparticles cross-section after laser annealing with the fundamental wavelength $\lambda_1 = 1064$ nm was $d = 70$ nm, and the height $h = 85$ nm. In the second case ($\lambda_2 = 532$ nm), after annealing with the same I values $d = 7$ nm, and $h = 5$ nm have been obtained. The thresholds of structural changes beginning and transformation of the SiO_x film were determined. The influence of laser intensity up to 100 MW/cm² on structural changes, surface nanocrystal concentration and conductivity was investigated. Laser induced changes of the structural, optical and electro-physical properties of SiO_x have been explained by generation, redistribution and agglomeration of interstitial Si atoms in solid phase due to the self-organization processes caused by the laser thermal shock effect in the core laser treatment without the need of super high-vacuum chambers and additional thermal heater.

Acknowledgment

The authors thanks to Dr. P. Litvin, and Dr. S. Zlobin for AFM and IR measurements.

References

1. Tiwari S., Rana F., Hanafi H., Hartstein A., Crabbe E.F., Chan K. A silicon nanocrystals based memory. *Appl. Phys. Lett.* 1996. **68**, No. 10. P. 1377–1379.
2. Hanafi H.I., Tiwari S., Khan I. Fast and long retention-time nanocrystal memory. *IEEE Trans. Electron. Devices.* 1996. **43**. P. 1553–1558.
3. She M., King T.-J. Impact of crystal size and tunnel dielectric on semiconductor nanocrystal memory

- performance. *IEEE Trans. Electron. Devices.* 2003. **50**, No. 9. P. 1934–1940.
4. Canham L. Gaining light from silicon. *Nature.* 2000. **408**. P. 411–412.
5. Ng W.L., Lourenço M.A., Gwilliam R.M., Ledain S., Shao G., and Homewood K.P. An efficient room-temperature silicon-based light-emitting diode. *Nature.* 2001. **410**(6825). P. 192–194.
6. Pavese L., Negro L. Dal, Mazzoleni C., Franzò G., Priolo F. Optical gain in silicon nanocrystals. *Nature.* 2000. **408**. P. 440.
7. Yun F., Hinds B.J., Hatatani S., Oda S., Zhao Q.X., Willander M. Study of structural and optical properties of nanocrystalline silicon embedded in SiO₂. *Thin Solid Films.* 2000. **375**. P. 137.
8. Koshizaki N., Hiroyuki H., Oyama T. XPS characterization and optical properties of Si/SiO₂, Si/Al₂O₃ and Si/MgO co-sputtered films. *Thin Solid Films.* 1998. **325**. P. 130.
9. Rinnert H., Vergnat M., Marchal G. Structure and optical properties of amorphous SiO_x thin films prepared by co-evaporation of Si and SiO. *Mater. Sci. Eng. B.* 2000. **484**. P. 69–70.
10. Bell F.G., Ley L. Photoemission study of SiO_x ($0 \leq x \leq 2$) alloys. *Phys. Rev. B.* 1988. **37**. P. 8383.
11. Bratus' O.L., Evtukh A.A., Lytvyn O.S., Voitovych M.V., Yuhymchuk V.O. Structural properties of nanocomposite SiO₂(Si) films obtained by ion-plasma sputtering and thermal annealing. *Semiconductor Physics, Quantum Electronics & Optoelectronics.* 2011. **14**. P. 247–255.
12. Rochet F., Dufour G., Roulet H., Pelloie B., Perrière J., Fogarassy E., Slaoui A., Froment M. Modification of SiO through room-temperature plasma treatments, rapid thermal annealings, and laser irradiation in a non-oxidizing atmosphere. *Phys. Rev. B.* 1988. **37**. P. 6468.
13. Gallas B., Kao C.-C., Fisson S., Vuye G., Rivory J., Bernard Y., Belouet C. Laser annealing of SiO_x thin films. *Appl. Surf. Sci.* 2002. **185**. P. 317–320.
14. Janotta A., Dikce Y., Schmidt M., Eisele C., Stutzmann M. Light-induced modification of a-SiO_x: Laser crystallization. *J. Appl. Phys.* 2004. **95**. P. 4060–4068.
15. Korchagina T.T., Gutakovskiy A.K., Fedina L.I., Neklyudova M.A., Volodin V.A. Crystallization of amorphous Si nanoclusters in SiO films using femtosecond laser pulse annealings. *J. Nanosci. Nanotechnol.* 2012. **12**. P. 8694–8699.
16. Gavrylyuk O.O., Semchyk O.Yu., Bratus O.L., Evtukh A.A., Steblova O.V., Fedorenko L.L. Study of thermophysical properties of crystalline silicon and silicon-rich silicon oxide layers. *Appl. Surf. Sci.* 2014. **302**. P. 213–215.
17. Pavese L. Routes toward silicon-based laser. *Mater. Today.* 2005. **8**, No. 1. P. 18–25.
18. Daniel C., Mucklich F., Liu Z. Periodical micro-nano-structuring of metallic surfaces by interfering

- laser beams. *Appl. Surf. Sci.* 2003. **208–209**. P. 317–321.
19. Medvid A., Fedorenko L. Optical excitation of the surface plasmon-polariton resonance in Zn nanoparticles formed by laser radiation in ZnO crystal. IX Intern. Conf. “*Topical Problems of Semiconductor Physics*”, Truskavets, Ukraine, May 16–20, 2016. P. 113–114.
 20. Shimizu A., Kanbara M., Hada M., and Kasuga M. ZnO green light emitting diode. *Jpn. J. Appl. Phys.* 1978. **17**. P. 1435.
 21. Lisovskii I.P., Litovchenko V.G., Lozinskii V.B., Frolov S.I., Flietner H., Fussel W., Schmidt E. IR study of short-range and local order in SiO₂ and SiO_x films. *J. Non-Crystalline Solids*. 1995. **187**. P. 91–95.
 22. Fedorenko L.L., Bolgov S.S., Malyutenko V.K. Activation of photoconductivity of InSb by laser radiation. *Ukr. J. Phys.* 1975. **14**, №.12. P. 2041–2044.
 23. Voronkov V.P., Gurchenok G.A. Impurity diffusion in semiconductors at laser annealing. *Phys. Technol. Semicond.* 1990. **24**. P. 1831–1834.
 24. Medvid’A., Fedorenko L.L., Snitka V. The mechanism of generation of donor centers in p-InSb by laser radiation. *Appl. Surf. Sci.* 1999. **142**. P. 280–285.
 25. Steblova O.V., Evtukh A.A., Bratus’O.L. et al. Transformation of SiO_x films into nanocomposite SiO₂(Si) films under thermal and laser annealing. *Semiconductor Physics, Quantum Electronics & Optoelectronics*. 2014. **17**, No. 3. P. 295–300.
 26. Hubner K. Chemical bond and related properties of SiO₂. VII. Structure and electronic properties of the SiO_x region of Si-SiO₂ interfaces. *physica status solidi (a)*. 1980. **61**, No. 2. P. 665–671.
 27. Kizjak A.Yu., Evtukh A.A., Steblova O.V., Pedchenko Yu.M. Electron transport through thin SiO₂ films containing Si nanoclusters. *J. Nano Res.* 2016. **39**. P. 169–177.